INSTITUTE OF PHYSICS PUBLISHING JOURNAL OF PHYSICS B: ATOMIC, MOLECULAR AND OPTICAL PHYSICS

J. Phys. B: At. Mol. Opt. Phys. **35** (2002) 1095–1102 PII: S0953-4075(02)31156-8

Electron-impact excitation of H-like Fe at high temperatures

C P Ballance[1], **N R Badnell**[2] **and K A Berrington**[1]

[1] School of Science and Mathematics, Sheffield Hallam University, Sheffield S1 1WB, UK
[2] Department of Physics and Applied Physics, University of Strathclyde, Glasgow G4 0NG, UK

Received 22 November 2001
Published 13 February 2002
Online at stacks.iop.org/JPhysB/35/1095

Abstract

There have been two previous works concerning the electron-impact excitation of H-like Fe employing the R-matrix technique. The calculations by Aggarwal and Kingston (Aggarwal K M and Kingston A E 1993 *Astrophys. J. Suppl. Ser.* **85** 187–95) were carried out non-relativistically in LS coupling while those of Kisielius *et al* (Kisielius R, Berrington K A and Norrington P H 1996 *Astron. Astrophys. Suppl. Ser.* **118** 157–62) allowed for relativistic effects by using the Dirac–Fock R-matrix method. There seems to general agreement about values of the effective collision strength up to about 10^6 K in temperature with Kisielius *et al*, but close inspection of the collision strengths for dipole transitions shows that they do not have the correct high-temperature form. We have carried out a new (Breit–Pauli) R-matrix calculation combined with close attention to high-energy behaviour and radiation damping (not included in the previous works). We present and discuss our results for improved effective collision strengths for the temperature range 10^6–$10^{8.5}$ K—the peak coronal fractional abundance of Fe^{25+} lies at $\approx 10^8$ K.

1. Introduction

The analysis of data returned by the new high-resolution x-ray satellites *Chandra* and *XMM-Newton* requires atomic collision data that, in general, is beyond the scope of that computed by the IRON Project (Hummer *et al* 1993). The RmaX Network[3] was formed to carry out extensive calculations of atomic data in the x-ray regime, using the radiation damped (Robicheaux *et al* 1995) R-matrix method (Berrington *et al* 1995). In particular, highly charged Fe systems exist at relatively low temperatures in photoionized plasmas, compared to coronal plasmas. These systems clearly illustrate the large contribution from Rydberg resonances on effective (Maxwellian-averaged) collision strengths, especially at lower temperatures (Ballance *et al* 2001). Also, resonances positioned just above an excitation threshold can be the dominant contribution to the effective collision strength at low temperatures. Similar observations were made by Kisielius *et al* (1996) following comparisons of their undamped R-matrix results for

[3] Available at http://amdpp.phys.strath.ac.uk/UK_RmaX/.

 © 2002 IOP Publishing Ltd Printed in the UK

Fe^{25+} with those of non-resonant calculations such as the Coulomb–Born–Oppenheimer (CBO) approach of Golden *et al* (1981) and Clarke *et al* (1982). However, we have observed that most of the high-temperature effective collision strengths of Kisielius *et al* (1996) decrease rapidly with increasing temperature whilst, asymptotically, they should increase logarithmically (or tend to a constant) for dipole (or non-dipole) allowed transitions. In particular, Burgess and Tully (1992) discuss the high-energy (temperature) behaviour of ordinary (effective) collision strengths in some detail.

Although the R-matrix method puts little restriction on the energy range spanned by the incident electron, it does require the diagonalization of ever larger Hamiltonians so as to increase the energy range. Beyond the final level included within a close-coupling (CC) expansion, there are no resonances and we would also expect little in the way of CC and distorted-wave effects in a highly charged ion. So, the computational effort of an R-matrix calculation is unnecessary and simpler approaches can be employed to obtain the high-energy contribution to effective collision strengths from ordinary collision strengths. In the case of dipole transitions, the infinite energy (temperature) ordinary (effective) collision strength is given by the Bethe approximation and it reduces to a simple formula involving the oscillator strength (Burgess and Tully 1992). Burgess *et al* (1997) extended this work to include the high-energy Born limits for the optically forbidden (allowed) transitions. Recently, Badnell and Thomas (see Whiteford *et al* (2001)) implemented and extended these multipole expressions within AUTOSTRUCTURE (Badnell 1997) for all multipoles. These limits cannot be expressed so concisely, and require the careful manipulation of Born integrals and fractional parentage coefficients together with the allowance for configuration mixing. We note that Burgess–Tully plots, in which the electron energy and collision strengths are scaled, indicate whether or not the infinite energy point for an allowed transition is being approached correctly. Consideration of the high-energy asymptotic behaviour of allowed transitions and utilization of the infinite energy limit point has enabled the results of R-matrix calculations to be extended into temperature ranges that were traditionally an order of magnitude too high to reach (see, for example, Whiteford *et al* (2001)). This means that population modelling into the 10^7–10^9 K temperature regime is feasible with such data.

Kisielius *et al* (1996), in regard to the scattering energies that they used in the electron-impact excitation of Fe^{25+}, state that 'the energy interval is chosen to be from 512.5 to 1000 Ry'. We assume that this (512.5) is a typing error as their table 1, relating the experimental levels of Erickson (1977), gives eigen-energies for the $2s_{1/2}$ and $2p_{1/2}$ levels to be 510.951 9822 and 510.994 9940 Ry, respectively. Furthermore, effective collision strengths to these levels are given in their table 5. The subsequent statement that 'this enables us to obtain Υ for temperature (sic) $T \leqslant 3 \times 10^7$' is overly optimistic, if no account is taken of collision strengths above 1000 Ry, and may explain why the effective collision strengths given in their table 5 begin to decay at their highest temperatures, for most transitions.

Consider the formula for a Maxwellian-averaged effective collision strength

$$\Upsilon_{ij} = \int_0^\infty \Omega_{ij} \exp\left(\frac{-E_j}{kT}\right) \mathrm{d}\left(\frac{E_j}{kT}\right), \tag{1}$$

where E_j represents the final-state free-electron energy, Ω_{ij} the collision strength for transition i–j, T the temperature and k the Boltzmann constant. To ensure closure in the integral of the slowly decaying exponential term, we require the ratio E_j/kT to be sufficiently large. For Ω a constant in energy—the asymptotic case of non-dipole-allowed transitions, a value of 7 for this ratio gives Υ to 0.1% accuracy. For the weakly divergent logarithmic Ω of dipole transitions, a somewhat larger ratio is required. At a temperature of 3×10^7 K, excitation of the $n = 4$ levels with an incident electron energy of 1000 Ry relative to the ground, as used by

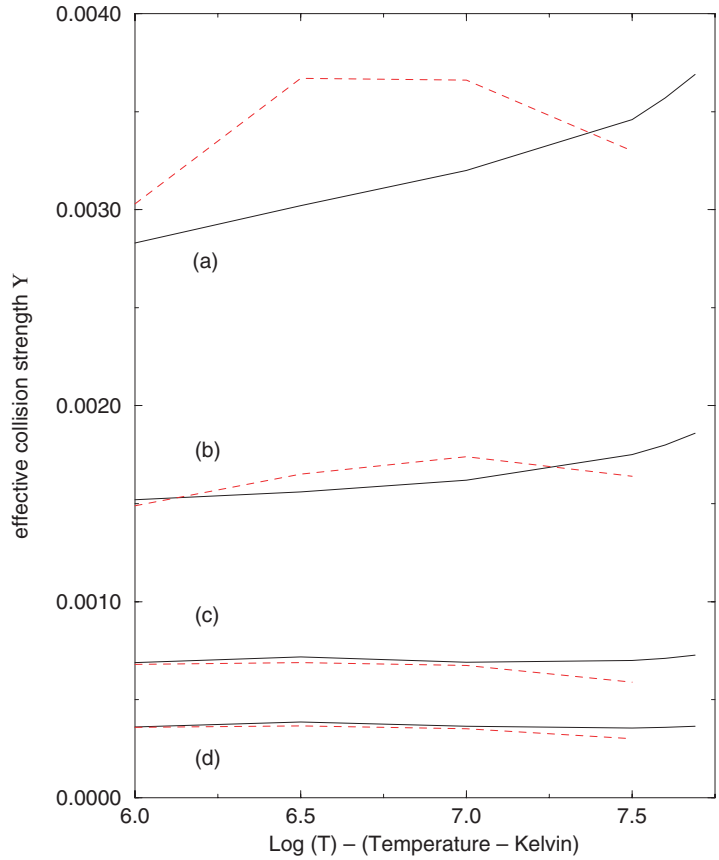

Figure 1. High-temperature effective collision strengths versus temperature (K) for dipole transitions from the ground state. The dotted curve denotes the results of Kisielius *et al* (1996) while the solid curve denotes our present results: for the, (a) $1s_{\frac{1}{2}}$–$2p_{\frac{3}{2}}$, (b) $1s_{\frac{1}{2}}$–$2p_{\frac{1}{2}}$, (c) $1s_{\frac{1}{2}}$–$3p_{\frac{3}{2}}$ and (d) $1s_{\frac{1}{2}}$–$3p_{\frac{1}{2}}$ transitions.

(This figure is in colour only in the electronic version)

Kisielius *et al* (1996), gives a ratio of about 1.9, and $e^{-1.9} \approx 0.15$. We find that it is necessary to consider contributions from up to ∼3000 Ry relative to the ground in this instance. As stated earlier, it is computationally burdensome and unnecessary to evaluate this contribution with explicit R-matrix calculations and we circumvent this problem by a linear interpolation of the scaled collision strengths between our highest calculated finite energy point and the infinite energy point, for each dipole and allowed transition, as classified by Burgess and Tully (1992).

2. Calculation

Our model again employs the R-matrix method (Berrington *et al* 1995) and we include the same $n \leqslant 5$ levels as included by Kisielius *et al* (1996). The atomic orbitals were generated by the structure package AUTOSTRUCTURE, as were the infinite energy Bethe and Born limits. The partial waves were treated in two different ways, in a similar vein to our Li-like Fe work (Ballance *et al* 2001). The low partial waves ($J = 0$–10), which include

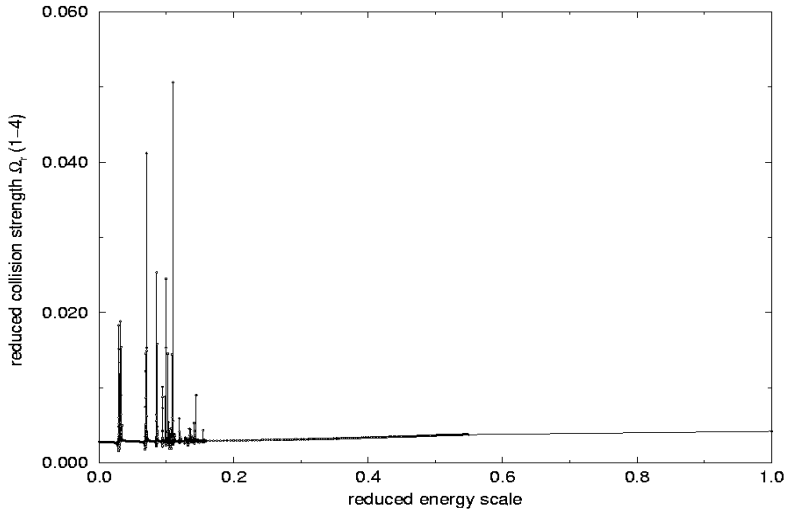

Figure 2. Burgess and Tully (1992) reduced plot for the $1s_{1/2}$–$2p_{3/2}$ dipole transition in which the collision strength is scaled by $\Omega_r = \Omega/\ln((E_j/E_{ij}) + e)$. E_j corresponds to the free-electron energy whilst E_{ij} represents the energy separation of the initial and final states. The free electron energy is scaled by $E_r = 1 - \ln(C)/\ln((E_j/E_{ij}) + C)$ where C is an arbitrary real constant, in this case we used $C = 2$.

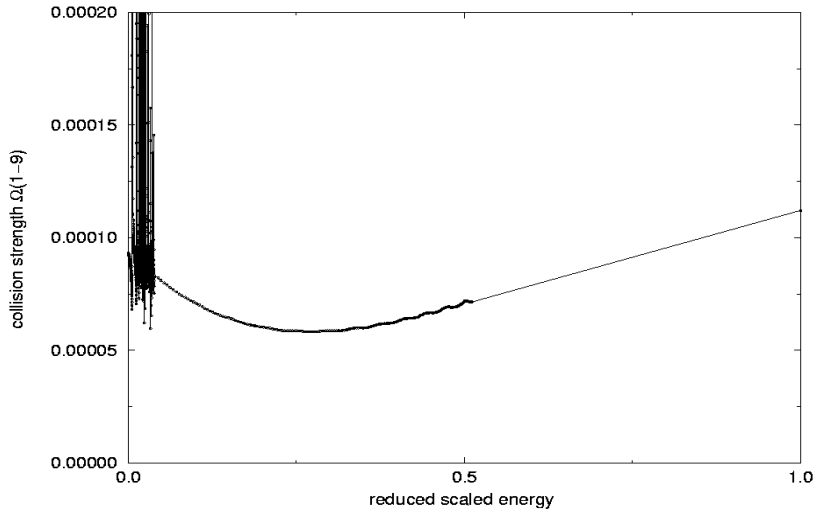

Figure 3. As figure 2, but for the quadrupole $1s_{1/2}$–$3d_{5/2}$ transition. Here only the free electron energy is scaled, this time by $E_r = (E_j/E_{ij})/(E_j/E_{ij} + C)$, $C = 2$ again.

rich Rydberg resonance structure, were obtained from a standard Breit–Pauli calculation (Berrington *et al* 1995). However, the $J = 11$–50 partial waves, required to ensure convergence for dipole transitions, were obtained via the intermediate coupling frame transformation approach of Griffin *et al* (1998). This entails transforming unphysical S- or K-matrices (within the framework of quantum defect theory) to a jK-coupling scheme before a further transformation, involving term-coupling coefficients, gives rise to intermediate coupling level-to-level excitation cross sections.

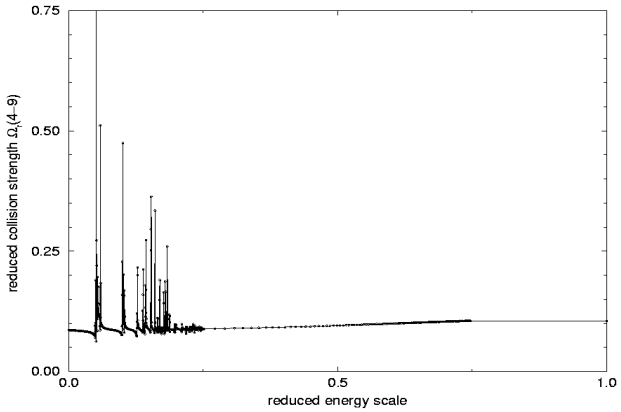

Figure 4. As figure 2, but for the $2p_{3/2}$–$3d_{5/2}$ dipole transition.

Our 25CC level calculation ($1s_{1/2}$–$5g_{9/2}$) used 56 continuum basis orbitals. This enabled us to generate collision strengths up 2000 Ry, to which we add the result for the infinite energy point for allowed transitions. We note that every transition is allowed, i.e. in the absence of configuration mixing and spin–orbit mixing, a non-vanishing Born or Bethe limit point exists. There are no weak 'forbidden' transitions that can only take place through mixing. Finally, radiation damping for the high-n members of a Rydberg series was introduced via a complex effective quantum number (Robicheaux *et al* 1995), which cancels some of the effective collision strength contribution from narrow resonances close to a threshold.

3. Discussion

We have calculated effective collision strengths over a temperature range of 10^6–10^9 K. The temperature range was extended beyond the $\log_{10}(T\,(\mathrm{K})) = 7.5$ presented in Kisielius *et al* (1996) because Arnaud and Raymond (1992) place the peak coronal abundance for Fe^{25+} at $\log_{10}(T\,(\mathrm{K})) \approx 8.1$. Note, higher temperature effective collision strengths can be determined by an interpolation that makes use of the infinite temperature limit point (Burgess and Tully 1992). This limit point is also present in the *adf04* data structure tabulation of our effective collision strengths under the atomic data and analysis structure format (Summers 1994, 1999).

If we consider a dipole transition, such as $1s_{1/2}$–$2p_{3/2}$, then we know that the scaled infinite energy Bethe limit for the effective collision strength is given by (Burgess and Tully 1992)

$$\frac{\Upsilon(1s_{\frac{1}{2}}\text{–}2p_{\frac{3}{2}})}{\ln(kT)} \rightarrow \frac{4w_i f_{ij}}{\Delta E_{ij}} \qquad \text{as} \quad kT \rightarrow \infty, \tag{2}$$

where w_i is the statistical weight of the initial state, f_{ij} the upward oscillator strength and ΔE_{ij} the energy separation of the levels. But, if we look along row 3 of table 5 of Kisielius *et al* (1996) we see that Υ reaches a maximum between $\log_{10}(T\,(\mathrm{K})) = 6.5$ and 7.0 and then decreases at $\log_{10}(T\,(\mathrm{K})) = 7.5$. This theme is consistent amongst nearly all of the dipole transitions. This is illustrated more clearly in figure 1 where effective collision strengths for dipole transitions from the ground state to the $2p_j$ and $3p_j$ levels are compared. There seems to be good argreement at $\log_{10}(T\,(\mathrm{K})) = 6.0$ before the Kisielius *et al* (1996) results rise slightly above our own, before decaying rapidly. Certainly, radiation damping could account for this discrepancy

Table 1. High-temperature effective collision strengths from the ground and first excited-state to the $n \leqslant 4$ levels ($a(-b)$ denotes $a \times 10^{-b}$).

	Temperature (K)							
Transition	10^{6}	$10^{6.5}$	$10^{7.0}$	$10^{7.5}$	$10^{7.80}$	$10^{8.0}$	$10^{8.2}$	$10^{8.5}$
$1s_{\frac{1}{2}}$–$2p_{\frac{1}{2}}$	1.52(−3)	1.56(−3)	1.62(−3)	1.77(−3)	2.02(−3)	2.29(−3)	2.67(−3)	3.42(−3)
$1s_{\frac{1}{2}}$–$2s_{\frac{1}{2}}$	1.14(−3)	1.11(−3)	1.10(−3)	1.08(−3)	1.08(−3)	1.08(−3)	1.09(−3)	1.10(−3)
$1s_{\frac{1}{2}}$–$2p_{\frac{3}{2}}$	2.83(−3)	3.01(−3)	3.18(−3)	3.49(−3)	3.99(−3)	4.53(−3)	5.27(−3)	6.76(−3)
$1s_{\frac{1}{2}}$–$3p_{\frac{1}{2}}$	3.57(−4)	3.60(−4)	3.42(−4)	3.47(−4)	3.79(−4)	4.17(−4)	4.71(−4)	5.81(−4)
$1s_{\frac{1}{2}}$–$3s_{\frac{1}{2}}$	2.48(−4)	2.52(−4)	2.32(−4)	2.16(−4)	2.11(−4)	2.08(−4)	2.07(−4)	2.07(−4)
$1s_{\frac{1}{2}}$–$3d_{\frac{3}{2}}$	1.30(−4)	1.37(−4)	9.65(−5)	6.42(−5)	5.41(−5)	5.10(−5)	5.03(−5)	5.27(−5)
$1s_{\frac{1}{2}}$–$3p_{\frac{3}{2}}$	6.90(−4)	7.19(−4)	6.92(−4)	7.06(−4)	7.72(−4)	8.51(−4)	9.62(−4)	1.19(−3)
$1s_{\frac{1}{2}}$–$3d_{\frac{5}{2}}$	1.87(−4)	1.85(−4)	1.32(−4)	9.07(−5)	7.80(−5)	7.45(−5)	7.43(−5)	7.86(−5)
$1s_{\frac{1}{2}}$–$4p_{\frac{1}{2}}$	1.42(−4)	1.32(−4)	1.24(−4)	1.25(−4)	1.35(−4)	1.48(−4)	1.66(−4)	2.03(−4)
$1s_{\frac{1}{2}}$–$4s_{\frac{1}{2}}$	1.00(−4)	9.23(−5)	8.34(−5)	7.82(−5)	7.60(−5)	7.49(−5)	7.41(−5)	7.37(−5)
$1s_{\frac{1}{2}}$–$4d_{\frac{3}{2}}$	6.24(−5)	4.86(−5)	3.54(−5)	2.69(−5)	2.40(−5)	2.32(−5)	2.32(−5)	2.44(−5)
$1s_{\frac{1}{2}}$–$4p_{\frac{3}{2}}$	2.55(−4)	2.52(−4)	2.48(−4)	2.57(−4)	2.80(−4)	3.07(−4)	3.45(−4)	4.22(−4)
$1s_{\frac{1}{2}}$–$4f_{\frac{5}{2}}$	2.61(−5)	1.61(−5)	7.30(−6)	3.16(−6)	1.96(−6)	1.47(−6)	1.14(−6)	8.58(−7)
$1s_{\frac{1}{2}}$–$4d_{\frac{5}{2}}$	7.62(−5)	6.51(−5)	5.03(−5)	3.95(−5)	3.56(−5)	3.45(−5)	3.47(−5)	3.68(−5)
$1s_{\frac{1}{2}}$–$4f_{\frac{7}{2}}$	2.59(−5)	1.58(−5)	7.40(−6)	3.41(−6)	2.21(−6)	1.70(−6)	1.36(−6)	1.07(−6)
$2p_{\frac{1}{2}}$–$3p_{\frac{1}{2}}$	1.35(−2)	1.39(−2)	1.34(−2)	1.32(−2)	1.33(−2)	1.34(−2)	1.35(−2)	1.36(−2)
$2p_{\frac{1}{2}}$–$3s_{\frac{1}{2}}$	1.83(−3)	1.99(−3)	1.55(−3)	1.31(−3)	1.42(−3)	1.59(−3)	1.84(−3)	2.33(−3)
$2p_{\frac{1}{2}}$–$3d_{\frac{3}{2}}$	4.70(−2)	5.05(−2)	5.72(−2)	7.52(−2)	9.38(−2)	1.09(−1)	1.27(−1)	1.58(−1)
$2p_{\frac{1}{2}}$–$3p_{\frac{3}{2}}$	5.76(−3)	5.74(−3)	4.28(−3)	3.18(−3)	2.87(−3)	2.77(−3)	2.73(−3)	2.74(−3)
$2p_{\frac{1}{2}}$–$3d_{\frac{5}{2}}$	1.19(−2)	1.13(−2)	7.88(−3)	5.09(−3)	4.08(−3)	3.66(−3)	3.38(−3)	3.15(−3)
$2p_{\frac{1}{2}}$–$4p_{\frac{1}{2}}$	2.74(−3)	2.59(−3)	2.45(−3)	2.40(−3)	2.41(−3)	2.42(−3)	2.44(−3)	2.47(−3)
$2p_{\frac{1}{2}}$–$4s_{\frac{1}{2}}$	7.21(−4)	5.61(−4)	3.94(−4)	3.13(−4)	3.13(−4)	3.33(−4)	3.68(−4)	4.44(−4)
$2p_{\frac{1}{2}}$–$4d_{\frac{3}{2}}$	8.99(−3)	9.18(−3)	1.00(−2)	1.25(−2)	1.50(−2)	1.71(−2)	1.95(−2)	2.37(−2)
$2p_{\frac{1}{2}}$–$4p_{\frac{3}{2}}$	1.87(−3)	1.54(−3)	1.12(−3)	8.13(−4)	7.04(−4)	6.59(−4)	6.30(−4)	6.08(−4)
$2p_{\frac{1}{2}}$–$4f_{\frac{5}{2}}$	2.29(−3)	1.97(−3)	1.85(−3)	2.19(−3)	2.57(−3)	2.84(−3)	3.10(−3)	3.44(−3)
$2p_{\frac{1}{2}}$–$4d_{\frac{5}{2}}$	3.16(−3)	2.58(−3)	1.82(−3)	1.17(−3)	8.92(−4)	7.64(−4)	6.74(−4)	5.96(−4)
$2p_{\frac{1}{2}}$–$4f_{\frac{7}{2}}$	1.97(−3)	1.41(−3)	8.69(−4)	5.20(−4)	4.00(−4)	3.50(−4)	3.17(−4)	2.90(−4)

alone. But, row 2 of table 5 (Kisielius *et al* 1996) indicates that between $\log_{10}(T(\mathrm{K})) = 6.0$ and 6.5 the effective collision strength for a monopole transition ($1s_{1/2}$–$2s_{1/2}$) increases faster than that for a dipole one ($1s_{1/2}$–$2p_{3/2}$), see row 3 of their table 5, which seems unusual. Furthermore, effective collision strengths for non-dipole (allowed) transitions tend to a constant at high temperatures (Burgess and Tully 1992). Again, the results in table 5 of Kisielius *et al* (1996) for many of these transitions fall-off quite rapidly at their highest temperatures.

In figures 2–4, we show Burgess and Tully (1992) reduced plots for a pair of dipole transitions as well as for a weak allowed quadrupole transition ($1s_{1/2}$–$3d_{5/2}$). Whilst these plots show that the collision strength for the (strong) dipole transitions reaches its asymptotic form rapidly, that for the weak quadrupole transition requires an energy 1000 Ry beyond the $3d_{5/2}$ threshold before it assumes its asymptotic form.

Table 2. High-temperature effective collision strengths from the $2s_{\frac{1}{2}}$ and $2p_{\frac{3}{2}}$ levels to the $n \leqslant 4$ levels.

	Temperature (K)							
Transition	10^6	$10^{6.5}$	$10^{7.0}$	$10^{7.5}$	$10^{7.8}$	$10^{8.0}$	$10^{8.2}$	$10^{8.5}$
$2s_{\frac{1}{2}}$–$3p_{\frac{1}{2}}$	5.97(−3)	6.06(−3)	6.82(−3)	9.94(−3)	1.35(−2)	1.66(−2)	2.02(−2)	2.64(−2)
$2s_{\frac{1}{2}}$–$3s_{\frac{1}{2}}$	1.36(−2)	1.29(−2)	1.29(−2)	1.34(−2)	1.38(−2)	1.41(−2)	1.43(−2)	1.45(−2)
$2s_{\frac{1}{2}}$–$3d_{\frac{3}{2}}$	1.20(−2)	1.25(−2)	1.24(−2)	1.37(−2)	1.51(−2)	1.60(−2)	1.68(−2)	1.77(−2)
$2s_{\frac{1}{2}}$–$3p_{\frac{3}{2}}$	9.34(−3)	1.05(−2)	1.25(−2)	1.88(−2)	2.57(−2)	3.18(−2)	3.88(−2)	5.08(−2)
$2s_{\frac{1}{2}}$–$3d_{\frac{5}{2}}$	1.77(−2)	1.82(−2)	1.84(−2)	2.05(−2)	2.26(−2)	2.40(−2)	2.52(−2)	2.66(−2)
$2s_{\frac{1}{2}}$–$4p_{\frac{1}{2}}$	1.42(−3)	1.36(−3)	1.44(−3)	1.95(−3)	2.54(−3)	3.07(−3)	3.69(−3)	4.77(−3)
$2s_{\frac{1}{2}}$–$4s_{\frac{1}{2}}$	2.39(−3)	2.37(−3)	2.35(−3)	2.44(−3)	2.51(−3)	2.56(−3)	2.60(−3)	2.64(−3)
$2s_{\frac{1}{2}}$–$4d_{\frac{3}{2}}$	2.38(−3)	2.14(−3)	1.95(−3)	1.96(−3)	2.05(−3)	2.12(−3)	2.19(−3)	2.29(−3)
$2s_{\frac{1}{2}}$–$4p_{\frac{3}{2}}$	2.51(−3)	2.49(−3)	2.75(−3)	3.81(−3)	5.02(−3)	6.08(−3)	7.33(−3)	9.49(−3)
$2s_{\frac{1}{2}}$–$4f_{\frac{5}{2}}$	1.69(−3)	1.48(−3)	1.27(−3)	1.21(−3)	1.23(−3)	1.25(−3)	1.27(−3)	1.29(−3)
$2s_{\frac{1}{2}}$–$4d_{\frac{5}{2}}$	3.47(−3)	3.21(−3)	2.95(−3)	2.97(−3)	3.10(−3)	3.22(−3)	3.32(−3)	3.46(−3)
$2s_{\frac{1}{2}}$–$4f_{\frac{7}{2}}$	2.37(−3)	2.00(−3)	1.71(−3)	1.64(−3)	1.66(−3)	1.69(−3)	1.71(−3)	1.73(−3)
$2p_{\frac{3}{2}}$–$3p_{\frac{1}{2}}$	7.16(−3)	6.45(−3)	4.67(−3)	3.43(−3)	3.09(−3)	2.98(−3)	2.92(−3)	2.89(−3)
$2p_{\frac{3}{2}}$–$3s_{\frac{1}{2}}$	3.97(−3)	4.08(−3)	3.13(−3)	2.82(−3)	3.17(−3)	3.61(−3)	4.19(−3)	5.28(−3)
$2p_{\frac{3}{2}}$–$3d_{\frac{3}{2}}$	2.36(−2)	2.43(−2)	2.17(−2)	2.19(−2)	2.45(−2)	2.72(−2)	3.05(−2)	3.65(−2)
$2p_{\frac{3}{2}}$–$3p_{\frac{3}{2}}$	3.30(−2)	3.41(−2)	3.20(−2)	3.07(−2)	3.06(−2)	3.07(−2)	3.08(−2)	3.08(−2)
$2p_{\frac{3}{2}}$–$3d_{\frac{5}{2}}$	9.55(−2)	1.02(−1)	1.13(−1)	1.45(−1)	1.78(−1)	2.07(−1)	2.40(−1)	2.96(−1)
$2p_{\frac{3}{2}}$–$4p_{\frac{1}{2}}$	1.97(−3)	1.55(−3)	1.12(−3)	8.16(−4)	7.09(−4)	6.65(−4)	6.37(−4)	6.14(−4)
$2p_{\frac{3}{2}}$–$4s_{\frac{1}{2}}$	1.33(−3)	1.04(−3)	7.54(−4)	6.40(−4)	6.72(−4)	7.34(−4)	8.24(−4)	1.00(−3)
$2p_{\frac{3}{2}}$–$4d_{\frac{3}{2}}$	6.02(−3)	5.19(−3)	4.31(−3)	3.95(−3)	4.09(−3)	4.35(−3)	4.73(−3)	5.46(−3)
$2p_{\frac{3}{2}}$–$4p_{\frac{3}{2}}$	7.62(−3)	7.02(−3)	6.35(−3)	5.99(−3)	5.90(−3)	5.87(−3)	5.86(−3)	5.83(−3)
$2p_{\frac{3}{2}}$–$4f_{\frac{5}{2}}$	3.34(−3)	2.52(−3)	1.75(−3)	1.37(−3)	1.32(−3)	1.33(−3)	1.36(−3)	1.41(−3)
$2p_{\frac{3}{2}}$–$4d_{\frac{5}{2}}$	1.93(−2)	1.91(−2)	1.99(−2)	2.38(−2)	2.81(−2)	3.18(−2)	3.61(−2)	4.36(−2)
$2p_{\frac{3}{2}}$–$4f_{\frac{7}{2}}$	5.96(−3)	4.79(−3)	4.12(−3)	4.48(−3)	5.06(−3)	5.48(−3)	5.89(−3)	6.38(−3)

In table 1, we present our effective collision strengths for all transitions from the ground and first excited state to the $n \leqslant 4$ levels over[4] $T = 10^6$–$10^{8.5}$ K. In table 2, we present similar results for excitations from the remaining $n = 2$ levels, but exclude transitions within the same n-shell. Our calculations give results for the allowed transitions which have the correct high-temperature form, but as we proceed to these higher temperatures the Υ integral relies ever more on the linear interpolation. Therefore, for weaker transitions whose approach to the asymptotic energy limit might not be so uniform, some overestimation or underestimation is inevitable. However, with regards to population modelling, it is important to have accurate rates for those transitions that are one to two orders of magnitude greater than these weak excitations.

[4] The full set of results for energy levels, dipole radiative rates and effective collision strengths over $T = 10^6$–10^9 K (including Born limits), tabulated in the ADAS *adf04* format (Summers 1994, 1999), is available via the WWW under http://www-cfadc.phy.ornl.gov/data_and_codes/. One of the authors (CPB) will be glad to provide all the effective collision strengths in electronic form to the interested reader. c.p.ballance@shu.ac.uk.

References

Aggarwal K M and Kingston A E 1993 *Astrophys. J. Suppl. Ser.* **85** 187–95
Arnaud M and Raymond J 1992 *Astrophys. J.* **398** 394–406
Badnell N R 1997 *J. Phys. B: At. Mol. Phys.* **30** 1–11
Ballance C P, Badnell N R and Berrington K A 2001 *J. Phys. B: At. Mol. Opt. Phys.* **34** 3287–300
Berrington K A, Eissner W B and Norrington P H 1995 *Comput. Phys. Commun.* **92** 290–420
Burgess A, Chidichimo M C and Tully J A 1997 *J. Phys. B: At. Mol. Opt. Phys.* **30** 33–57
Burgess A and Tully J A 1992 *Astron. Astrophys.* **254** 436–53
Clark R E H, Sampson D H and Goett S J 1982 *Astrophys. J. Suppl. Ser.* **49** 545–54
Erickson G W 1977 *J. Phys. Chem. Ref. Data* **6** 831–69
Golden L B, Clarke R E H, Goett S J and Sampson D H 1981 *Astrophys. J. Suppl. Ser.* **45** 603
Griffin D C, Badnell N R and Pindzola M S 1998 *J. Phys. B: At. Mol. Opt. Phys.* **31** 3713–27
Hummer D G, Berrington K A, Eissner W, Pradhan A K, Saraph H E and Tully J A 1993 *Astron. Astrophys.* **279** 298–309
Kisielius R, Berrington K A and Norrington P H 1996 *Astron. Astrophys. Suppl. Ser.* **118** 157–62
Robicheaux F, Gorczyca T W, Pindzola M S and Badnell N R 1995 *Phys. Rev.* A **52** 1319–33
Summers H P 1994 *JET Joint Undertaking Report* JET-IR(94)06
Summers H P 1999 *ADAS User Manual Version 2.1* webpage http://adas.phys.strath.ac.uk
Whiteford A D, Badnell N R, Ballance C P, O'Mullane M G, Summers H P and Thomas A L 2001 *J. Phys. B: At. Mol. Opt. Phys.* **34** 3179–91